http://dx.doi.org/10.21611/qirt.1996.018

Experimental and numerical investigations of thermo-mechanical field coupling effects during crack evolution

by J. Vogel[1], J. Auersperg[2], M. Dost[2], W. Faust[3] and B. Michel[2,3]

[1] TU Chemnitz-Zwickau, Institut für Mechanik, D-09107 Chemnitz; [2] Chemnitzer Werkstoffmechanik GmbH, Postfach 344, D-09003 Chemnitz; [3] Fraunhofer Institut für Zuverlässigkeit und Mikrointegration (IZM) Berlin, Gustav-Meyer-Allee 35, D-13355 Berlin; Germany

Abstract

A hybrid method combining infrared metrology and numerical simulation enables the investigation of thermo-mechanical field coupling effects in the vicinity of the crack tip. The temperature fields are analysed as a function of the loading rate, the specimen geometry and the crack evolution using infrared thermography. The experimental results are used for adjusting and verifying FE-calculations.

1. Introduction

Large plastic deformations occur during all stages of the fracture process in the vicinity of the crack tip especially of ductile materials. Thereby, up to 90% of the plastic work rate is dissipated as heat. If the strain rate is high enough so that the heat transfer is negligible a temperature rise can be proved. It should be noted that the plastic zone changes its position during crack propagation and acts as a moving, distributed heat source.

Among others ZEHNDER and ROSAKIS [1] have analysed the temperature rise in high speed experiments at modified CT-specimens. They have measured an increase of temperature of over 425 °C in 4340 steel and Beta-C titanium for crack propagating rates up to 1200 m/s. On the one hand, such a local temperature rise is connected with significant thermal strains in addition to the mechanical deformations. On the other hand, these high temperatures influence the mechanical properties particularly at the crack tip such as Young's modulus, yield stress and fracture parameters including the constitutive equations describing the mechanical behaviour. Consequently, a feed back is obtained to the mechanical stress and strain fields.

This sophisticated coupled field problem can be only interactively solved using suitable numerical methods like FEM because closed solutions for coupling of internal strain rate and thermal effects do not exist. Nevertheless, a number of theoretical estimations for the temperature rise around a moving crack tip have been performed, see e.g. [2-4]. But the values predicted for the temperature development can differ in a wide range according to the details of the models employed. For that reason, precise experimental data are required to fill this lack, to verify the theoretical results and to adjust the numerical calculations.

The coupling of numerical simulation and quantitative temperature field analysis by infrared thermography offers a favourable solution to investigate the influence of heat generation on the deformation behaviour and on the fracture toughness during the fracture process.

2. Crack temperature field analysis

Various measurement techniques are used to determine the temperature distributions generated by the heat development resulting from reversible and irreversible deformation processes. The temperature caused by the heat dissipation due to large deformations near the crack tip was measured e.g. by thermocouples, resistance temperature conductors, liquid crystal foils or infrared metrology [5-6]. In the case of a fast crack propagating at over 1000 m/s the temperature rise is recorded by IR-detectors at discrete points with an extremely high sampling rate by means of 10 MHz storing the voltage output in digital oscilloscopes [1]. If the crack rate $\dot{a}$ is lower, imaging IR-systems are suitable to analyse both the global and local temperature fields during the crack evolution with a sufficient frame rate up to 30 Hz and a high spatial resolution [7-8].

http://dx.doi.org/10.21611/qirt.1996.018

2.1. Experimental technique

A plasticity-type steel X2CrNi1911 was chosen due to its high ductility with a ratio between tensile strength and yield stress of nearly three and a comparable low heat conductivity. The temperature dependence of Young`s modulus and yield stress are given in Table 1.

temperature T	[°C]	20	50	100	150	200	250	400
Young`s modulus E	[GPa]	200		194		186		172
yield stress $R_{p0.2}$	[MPa]	180	162	147	132	118	108	89

Table 1. Temperature dependent mechanical properties of X2CrNi1911 (DIN 17440)

Single edge notched tension (SENT) and compact tension (CT) specimens were investigated. The geometry of the precracked CT-specimens corresponds to ASTM E399-90, figure 1. The starter notch is cut by spark erosion. The fatigue cracks are generated in a high frequency pulsator at a frequency of 70±3 Hz and a load ratio $R = F_u/F_o = 0.1$ at an average load level of 2.75 kN. The initial crack length a_0 realised satisfies the condition $0.45 \leq a_0/W \leq 0.55$. Figure 2 shows the crack profile of a CT-specimen broken after crack initiation.

The experiments were carried out displacement-controlled in an electromechanical testing machine with a maximum load of 100 kN, figure 3. The machine speed was varied in a wide range up to a maximum speed of v_{ms} = 16.7 mm/s. To avoid additional loads such as bending and torsion moments, the specimens are mounted on girbals with ball-and-socket bearings. The crack opening displacement was measured by a COD-clip MTS 632.03F-30 with a maximum travel of 12mm and the signals are formed by a measuring amplifier MGC from HBM.

Two short wave IR-systems, AGEMA 870 and TVS 2000 from NIPPON AVIONICS, are used in the experiments. The sensitivity of 0.1 K at 30 °C and the image field with more than 100 lines/frame and 250 sample/line allow good recording conditions for the temperature. A thin TETENAL coating on the specimens surface under investigation ensures a reproducible emission coefficient of $\varepsilon \approx 0.9$. Caused by its high toughness and adhesion the coating does not tear.

2.2. Results

Figure 4 shows the temperature rise as a function of the crack rate provided that the specimens have the same geometry. Even a low machine speed v_{ms} = 1 mm/s leads to an elliptical temperature distribution with a maximum of T_{max} = 50.1 °C at the crack tip. Owing to the dominance of the heat conductivity only a comparable low temperature difference of 20 K is found. But the dissipated plastic work energy generates an essentially higher crack tip temperature in a shorter time for a more adiabatic process at the maximum speed v_{ms} = 16.7 mm/s. Due to the temperature maximum of T_{max} = 155 °C at the crack tip the yield stress is locally reduced to approximately 70%. The dark areas far from the crack tip are on the level of the surrounding temperature. That means, no heat is generated in this volume region or transmitted to that.

Comparing specimens with different thicknesses loaded at the same machine speed, the temperature maximum near the crack tip, at the same time, figure 5, does not distinguish between the different specimens. However, the temperature fields differ clearly in their shape. This influence of the thickness can be interpreted by differences in the thermal transport mechanisms and the multiaxial stress field at the crack tip. Furthermore, a comparable slight temperature increase is observed in the compressed region opposite the crack. Further results are extensively discussed in [8].

3. FE-calculation

Temperature rise during crack growth in ductile materials occurs because the plastic work rate is converted into heat. Assuming adiabatic conditions and neglecting thermoelastic effects

http://dx.doi.org/10.21611/qirt.1996.018

this temperature rise $\Delta T(t)$ can be written in a first approximation as

$$\rho\, c_p\, \Delta T(t) = \int_{-\infty}^{t} \beta \sigma_{ij}(\tau) \dot{\varepsilon}_{ij}^{pl}(\tau) d\tau \tag{1}$$

with the material density ρ, the specific heat c_p, the weighting factor $\beta \approx 0.85...1.0$, the stress tensor σ_{ij} and the strain tensor ε_{ij}. The heat conduction equation is extended by a heat source term $\beta\sigma_{ij}\dot{\varepsilon}_{ij}^{pl}$

$$\kappa \nabla^2 T - \rho c_p \dot{T} = -\beta \sigma_{ij} \dot{\varepsilon}_{ij}^{pl} = -\dot{W}^{pl} \tag{2}$$

with the heat conduction coefficient κ. In order to determine the temperature distribution the thermal problem is simultaneously solved with the mechanical problem. Finally, the FE-calculation has to take into account the temperature dependence of the material properties. It has to be noted that an elastic-viscoplastic material behaviour is assumed.

The in-house FE-code ASTOR used to solve the coupled thermo-mechanical problem performs adaptive meshing and time stepping algorithms [9].

Figure 6 shows the heat propagation during crack blunting and crack propagation. The evolution of the magnitude of temperature versus the time is pointed out in figure 7. The influence of the temperature rise near the growing crack tip on the fracture parameters is demonstrated in [9] by means of the ΔT^*-integral from BRUST et al. [10]

$$\Delta T_k^* = \int_{\Gamma} \left[-\Delta W n_k - \left(\sigma_{ij} + \Delta\sigma_{ij}\right) n_i \Delta u_{i,k} - \Delta\sigma_{ij} n_j u_{i,k} \right] d\gamma + \ldots$$
$$\ldots + \int_{\Omega-\Omega_\varepsilon} \left[\Delta\sigma_{ij}\left(\varepsilon_{ij,k} + \frac{1}{2}\Delta\varepsilon_{ij,k}\right) - \Delta\varepsilon_{ij}\left(\sigma_{ij,k} + \frac{1}{2}\Delta\sigma_{ij,k}\right) \right] d\omega \tag{3}$$

The comparison between the calculated and measured temperature fields allows an adjustment of the heat flux conditions through the boundary of the specimen especially through the crack surfaces and the verification of the models used in the numerical simulations.

4. Acknowledgement

This work was performed with the support of the Deutsche Forschungsgemeinschaft (DFG) within the program „Yield fracture mechanics" under the number Mi 362/2-3. This support is gratefully acknowledged. Furthermore, the authors thank Dr. Wobst, in memoriam, and his co-workers from the Bundesanstalt für Materialforschung und -prüfung Berlin for generating the fatigue cracks.

REFERENCES

[1] ZEHNDER (A.T.) & ROSAKIS (A.J.). - *Temperature rise at the tip of dynamically propagating cracks: Measurements using high-speed infrared detectors.* Epstein (J.S.) ed., Experimental techniques in fracture mechanics. New York, VCH Publishers Inc., 1993, p. 125-169.

[2] RICE (J.R.) & LEVY (N.). - *Local heating by plastic deformation at a crack tip.* Argon (A.S.) ed., The physics of strength and plasticity. Cambridge, Academic Press, 1969, p. 277-293.

[3] WEICHERT (R.) & SCHÖNERT (K.). - *On the temperature rise at the tip of a fast running crack.* Journ. Mech. Phys. Solids 22, 1974, p. 127-133.

[4] HENNIG, K.; MICHEL (B.) & SOMMER (P.). - *Crack tip temperature fields in viscoplastic materials.* Proc. 6th Int. Conf. on Fracture (ICF6) - Vol. 4, New Dehli, 1984, p. 2587-2594.

[5] DÖLL (W.). - *An experimental study of the heat generated in the plastic region of a running crack in different polymeric materials.* Eng. Frac. Mech. 5, 1973, p. 259-268.

[6] KLEMM, (W.). - *Thermomechanical measuring proceedings for characterising the material resistance against fast fracture.* VDI-Berichte 679, 1988, p. 185-202.

[7] CHRYSOCHOOS (A.) & DUPRE (J.C.). - *An infrared set-up for continuum thermomechanics.* Eurotherm Series 27 - QIRT'92, Paris, 1992, p. 129-134.

http://dx.doi.org/10.21611/qirt.1996.018

[8] AUERSPERG (J.), VOGEL (D.), VOGEL (J.), DOST (M.) & FAUST (W.). - *Coupled crack tip temperature approach.* Michel (B.) ed., Deutsche Forschungsgemeinschaft, Bonn ,1994, Report-No. Mi 362/2-3.

[9] AUERSPERG (J.), DUDEK (R.) & MICHEL (B.). - *Untersuchungen zum thermisch-mechanischen Feldkopplungseffekt bei quasistatischer Rißausbreitung und Anwendung in der Mikrosystemtechnik.* Proc. of the ABAQUS user meeting, Ulm, 1995.

[10] BRUST (F.M.), NISHIOKA (T.), ATLURI (S.N.) & NAKAGAKI (M.). - *Further studying on elastic-plastic stable fracture utilizing the T'-integral.* Eng. Frac. Mech. 22, 1985, p. 1079-1103.

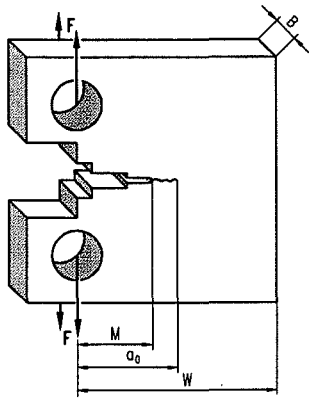

width	B = 50 mm
thickness	W = 6...12.5 mm
initial crack length	a_0 = 25 ± 2 mm

Fig. 1. CT-specimen (geometry according to ASTM E399-90)

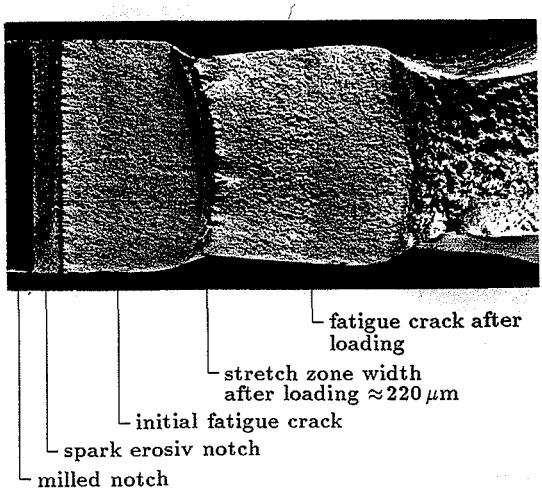

Fig. 2. Crack profile of a CT-specimen broken after crack initiation

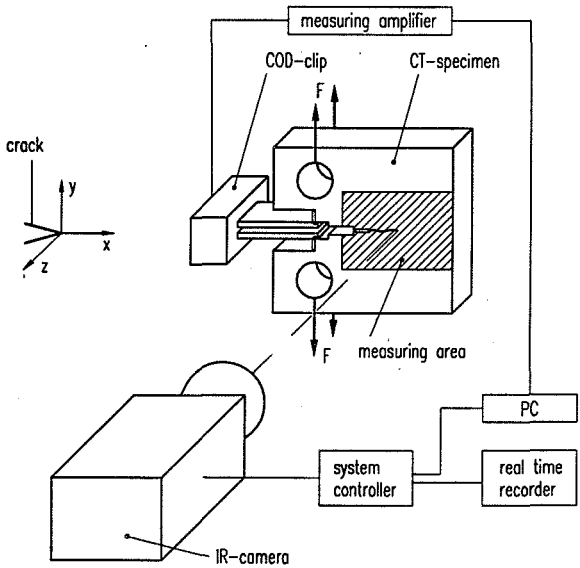

Fig. 3. Experimental set-up

http://dx.doi.org/10.21611/qirt.1996.018

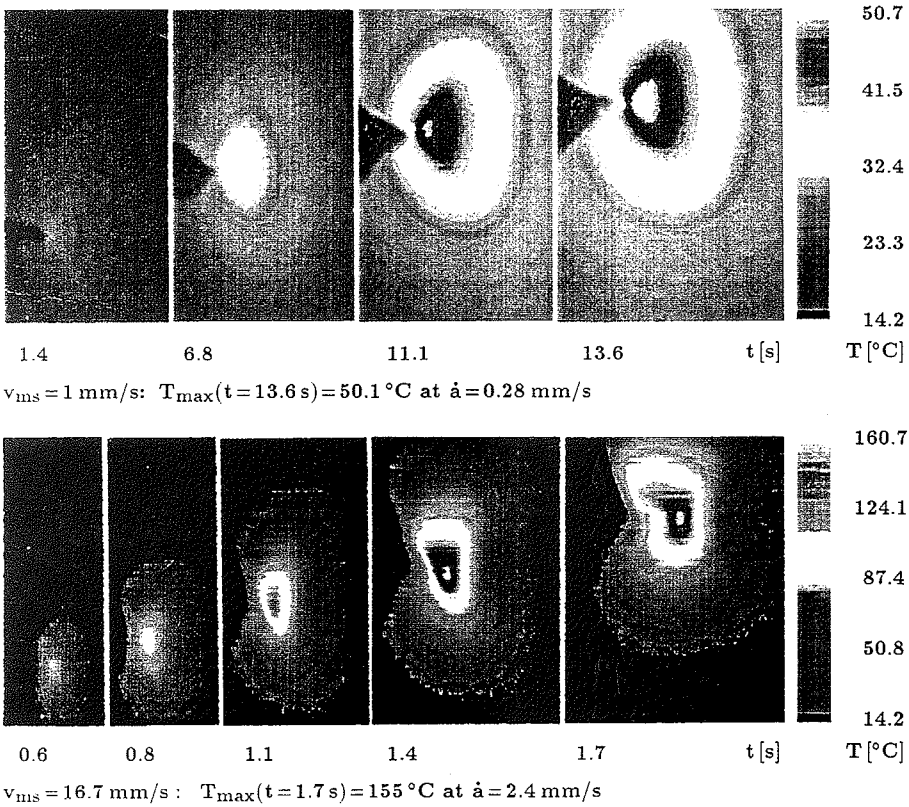

Fig. 4. Time dependent temperature rise near the crack tip on CT-specimens at two speeds v_{ms}

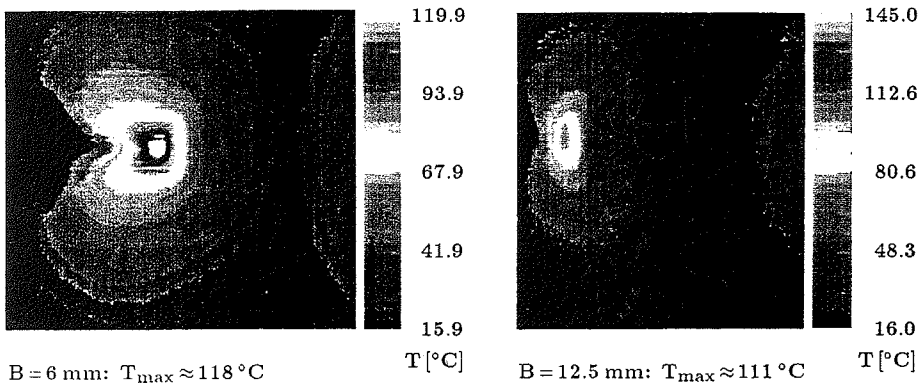

Fig. 5. Temperature distribution in the vicinity of the crack tip on CT-specimens as a function of the thickness B at the same time t = 1.7 s; v_{ms} = 10 mm/s ($\dot{a}$ = 1.8 mm/s)

http://dx.doi.org/10.21611/qirt.1996.018

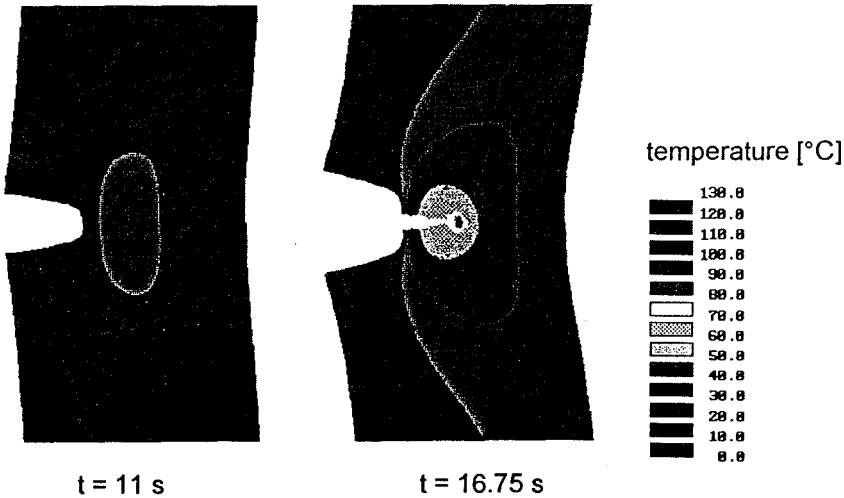

Fig. 6. Temperature field of the deformed SENT-specimen in the stage of crack blunting and crack propagation

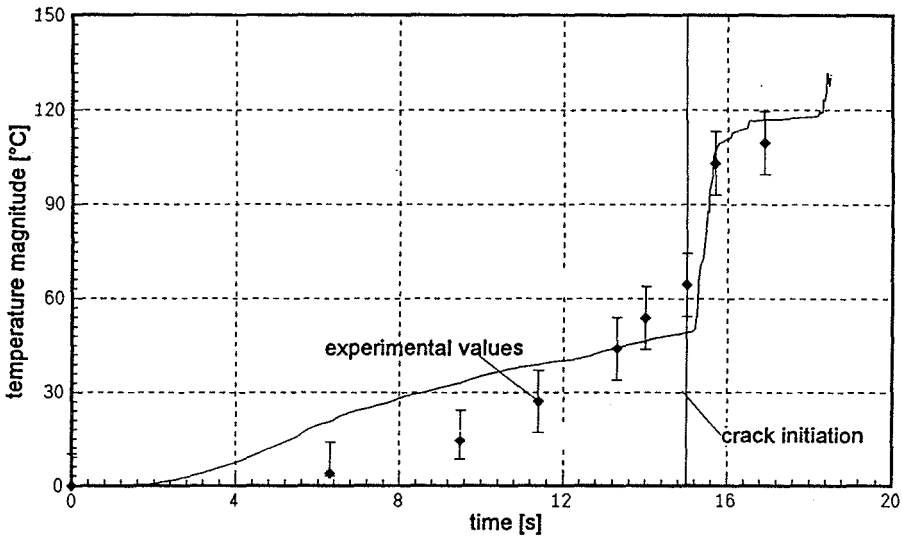

Fig. 7. Time dependent development of temperature maximum during the whole process